coatings

MDPI

Communication

Water-Processed Organic Solar Cells with Open-Circuit Voltages Exceeding 1.3V

Varun Vohra [1,*], Shunsuke Shimizu [2] and Yuko Takeoka [2,*]

[1] Department of Engineering Science, University of Electro-Communications, Chofu, Tokyo 182-8585, Japan
[2] Department of Materials & Life Sciences, Sophia University, Chiyoda, Tokyo 102-8554, Japan; s-shimizu-t79@eagle.sophia.ac.jp
* Correspondence: varun.vohra@uec.ac.jp (V.V.); y-tabuch@sophia.ac.jp (Y.T.)

Received: 4 April 2020; Accepted: 22 April 2020; Published: 24 April 2020

Abstract: Conjugated polyelectrolytes are commonly employed as interlayers to modify organic solar cell (OSC) electrode work functions but their use as an electron donor in water-processed OSC active layers has barely been investigated. Here, we demonstrate that poly[3-(6′-*N*,*N*,*N*-trimethyl ammonium)-hexylthiophene] bromide (P3HTN) can be employed as an electron donor combined with a water-soluble fullerene (PEG-C_{60}) into eco-friendly active layers deposited from aqueous solutions. Spin-coating a poly(3,4-ethylenedioxythiophene):polystyrene sulfonate (PEDOT:PSS) layer prior to the P3HTN:PEG-C_{60} active layer deposition considerably increases the open-circuit voltage (V_{oc}) of the OSCs to values above 1.3 V. Along with this enhanced V_{oc}, the OSCs fabricated with the PEDOT:PSS interlayers exhibit 10-fold and 5-fold increases in short-circuit current density (J_{sc}) with respect to those employing bare indium tin oxide (ITO) and molybdenum trioxide coated ITO anodes, respectively. These findings suggest that the enhanced J_{sc} and V_{oc} in the water-processed OSCs using the PEDOT:PSS interlayer cannot be solely ascribed to a better hole collection but rather to ion exchanges taking place between PEDOT:PSS and P3HTN. We investigate the optoelectronic properties of the newly formed polyelectrolytes using absorption and photoelectron spectroscopy combined with hole transport measurements to elucidate the enhanced photovoltaic parameters obtained in the OSCs prepared with PEDOT:PSS and P3HTN.

Keywords: conjugated polyelectrolytes; frontier orbitals; organic semiconductors; organic solar cells; sustainable fabrication

1. Introduction

Over the past decades, several solution-processable photovoltaic technologies have been introduced to replace the state-of-the-art silicon solar cells, which require a large energy input during their fabrication [1–4]. Among the alternative low carbon footprint solutions, organic solar cells (OSCs) exhibit a strong potential for facile integration into a variety of flexible and semitransparent technologies [1,5–8]. However, during their conventional active layers processing, an enormous amount of chlorinated solvent waste is generated, which is dangerous for the human health and the environment [5,9]. To mitigate the negative impact of OSC fabrication on the environment, several strategies have been investigated recently, which include the use of "greener" solvents such as limonene or nonhalogenated benzene derivatives [10–13], the synthesis of new organic semiconductors that are readily soluble in polar solvents [14], the introduction of water-based organic semiconductor inks [15–17], and the development of new coating processes to reduce wastes [18,19]. Although high power conversion efficiencies (*PCE*s) well over 10% can be achieved with OSC active layers processed from the abovementioned nonhalogenated solvents, the safety data sheets of these solvents indicate that they remain relatively hazardous to the environment [10,11]. Therefore, they do not represent a

remarkable improvement in terms of eco-friendliness with respect to conventional processing from chlorinated aromatic solvents. On the other hand, aqueous inks are generally produced through time-consuming processes that initially require dissolving the molecules in hazardous solvents. Materials that are readily soluble in water or alcohols thus seem to be the most promising strategy for the green fabrication of OSCs. Furthermore, several examples of conjugated polymers functionalized with oligo(ethylene glycol) suggest that high photovoltaic performances and *PCE*s can be achieved in water-processed OSCs [14].

Polymers composed of a conjugated backbone and pendant ionic chains are readily soluble in water/alcohols. These polyelectrolytes have received considerable attention as interlayer materials to tune the work function of OSC electrodes but have rarely been investigated as water/alcohol-processable active materials [20]. This is mainly due to the fact that the ions in the pendant chains will strongly respond to the applied bias [21]. Owing to their peculiar optoelectronic properties, polythiophenes and their derivatives have been extensively studied and are often considered state-of-the-art electron donors for OSC active layers [22,23]. In fact, poly[3-(6′-*N*,*N*,*N*-trimethyl ammonium)-hexylthiophene] bromide (P3HTN), a water-soluble polythiophene-based conjugated polycation, has been investigated both as an interlayer and active material for OSCs [24–26]. Lanzi et al. fabricated the active layer using P3HTN combined with the [6,6]-phenyl C_{61} butyric acid methyl ester (PCBM). As PCBM is a fullerene C_{60} derivative that is not soluble in water, the molecule was sonicated in water prior to deposition to achieve OSCs with decent *PCE*s around 3% [26]. However, such a fabrication process considerably reduces the reproducibility of the devices. For instance, we could not reproduce these results in our laboratory using the same procedure.

Here, we explore an alternative approach to fabricating OSCs using P3HTN-based active layers deposited from water. To ensure that OSCs can be fabricated in a reproducible manner, we replace PCBM with a water-soluble C_{60} functionalized with polyethylene glycol (PEG-C_{60}). Although the PCE of P3HTN:PEG-C_{60} OSCs is significantly lower than that of the previously reported P3HTN:PCBM OSCs, a very high open-circuit voltage (V_{oc}) with a value exceeding 1.3 V is produced when the active layer is deposited onto a poly(3,4-ethylenedioxythiophene):polystyrene sulfonate (PEDOT:PSS) hole transporting layer. We attribute this large increase in V_{oc} to ion exchanges occurring between P3HTN and PEDOT:PSS leading to the formation of new ionic complexes with enhanced optoelectronic properties.

2. Materials and Methods

P3HTN was synthesized from the quarternization reaction of the precursor polymer, poly[3-(6-bromohexyl)thiophene]] (PBHT) with trimethylamine. PBHT was produced from 2,5-dibromo-3-(6-bromohexyl)thiophene using the Kumada catalyst transfer polycondensation method, which is widely used for π-conjugated polymers synthesis [27,28]. The molecular weight of PHBT was determined by gel permeation chromatography (Tosoh HLC-8320GPC, Tokyo, Japan) equipped with two Shodex LF-804 columns. Measurements were carried out at 40 °C using tetrahydrofuran as the eluent at a flow rate of 1.0 mL·min^{-1}. Molecular weights were estimated from a calibration curve constructed using polystyrene standards. The number average molecular weight of PBHT was 3957 g·mol^{-1} with a polydispersity index of 1.39. This resulted in a number average molecular weight of P3HTN of 4774 g·mol^{-1} after the quartenization reaction. PEG-C_{60} and PEDOT:PSS (Clevios AI4083) were purchased from Solenne and Heraeus, respectively.

Patterned indium tin oxide (ITO) substrates (Atsugi Micro) were cleaned by sequential sonication in acetone, detergent, deionized water, isopropanol, and hot isopropanol followed by the UV/ozone surface treatment for 5 min. Some ITO substrates are coated with the PEDOT:PSS suspension at 4000 rpm for 30 s followed by thermal annealing in air at 200 °C for 10 min or with 10 nm of molybdenum trioxide (MoO_3) deposited in a high vacuum. P3HTN and PEG-C_{60} are blended in deionized water using P3HTN concentrations of 3 mg·mL^{-1} and with an optimized P3HTN:PEG-C_{60} ratio of 1:0.8. These solutions are deposited on ITO, PEDOT:PSS-coated ITO, or MoO_3-coated ITO substrates at

300 rpm for 40 s followed by a short 2 s step at 750 rpm. After annealing these active layers at 100 °C for 10 min to entirely remove any trace of water, the OSCs are finalized by sequentially evaporating 1.5 nm of cesium carbonate and 75 nm of silver (Ag) in a high vacuum. The photovoltaic characteristics of the devices were measured when exposed to a solar simulator (AM1.5G) at 1 sun (100 mW·cm^{-2}) using a Keithley 2401 sourcemeter (Cleveland, OH, USA). The reported data corresponds to the average values obtained from eight devices, which is presented together with the standard deviation of their *PCE*.

Two different types of hole only devices were fabricated. First, we deposited the P3HTN layer from a 3 mg·mL^{-1} aqueous solution onto ITO substrates coated with a 10 nm MoO_3 layer. The P3HTN layer was then annealed at 100 °C for 10 min followed by sequential evaporation of MoO_3 (10 nm) and Ag (75 nm). The second type of hole only devices were prepared with PEDOT:PSS. The PEDOT:PSS and P3HTN layers were deposited and annealed as described above. After a second layer of PEDOT:PSS aqueous dispersion containing 0.5 vol% of Triton-X (Sigma-Aldrich) was spin-coated at 1600 rpm on top of the P3HTN layer and annealed at 100 °C for 10 min, the devices were finalized by evaporating 75 nm of Ag. The current-voltage (*J*-*V*) characteristics of the hole only devices were measured using a Keithley 2401 sourcemeter and fitted to the space-charge limited model equation described in Equation (1) below to extract the hole mobility (μ):

$$J = \frac{9}{8}\varepsilon_0\varepsilon_r\mu\frac{V^2}{L^3} \quad (1)$$

where ε_0, ε_r and L correspond to the permittivity of free space, the relative dielectric constant, and the active layer thickness, respectively.

Ultraviolet (UV)/visible absorption spectra were acquired using a Shimadzu UV-3100PC spectrophotometer (Kyoto, Japan). UV photoelectron spectroscopy (UPS) spectra were acquired with a Jeol JPS-9200 photoelectron spectrometer (Tokyo, Japan).

3. Results and Discussion

A schematic representation of the device architectures and the active materials studied here can be found in Figure 1a. OSCs employing bare ITO, ITO/MoO_3, and ITO/PEDOT:PSS anodes are referred to as OSC-Ref, OSC-MoO_3, and OSC-PEDOT:PSS, respectively. The addition of a hole collecting/electron blocking layer such as PEDOT:PSS or MoO_3 at the active layer/anode interface of OSCs is a well-known strategy to improve their photovoltaic performances through reduced leak currents [29].

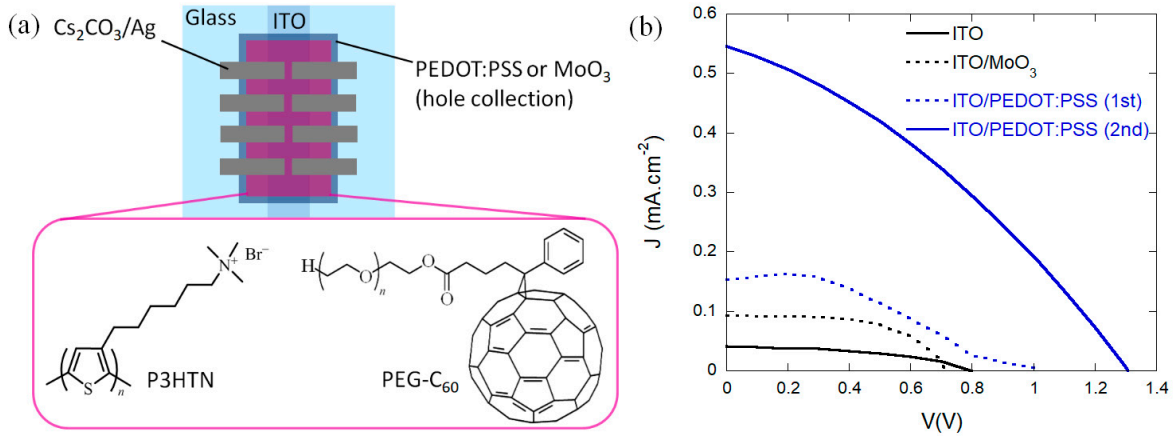

Figure 1. (**a**) Schematic representation of the organic solar cell (OSC) architecture and the molecular structures of the active materials; (**b**) current density-voltage (*J*-*V*) characteristics of OSC-Ref (solid black line), OSC-MoO_3 (dashed black line), with the first (dashed line) and second (solid line) scans of OSC-PEDOT:PSS (blue lines) under 1 sun.

As P3HTN and PEG-C_{60} have a limited solubility in water, the water-processed active layers are extremely thin with thicknesses around 20 nm. As a result, low short-circuit current densities (J_{sc})

are produced in OSC-Ref due to the small amount of sunlight absorbed by the devices (Figure 1b and Table 1). As expected, the addition of the charge selective layer in OSC-MoO_3 leads to an increase in J_{sc} from 0.041 mA·cm^{-2} for OSC-Ref to 0.093 mA·cm^{-2} for OSC-MoO_3. Additionally, the better charge collection efficiency is reflected through an enhancement of the fill factor (*FF*) to values around 60% in OSC-MoO_3. These *FF* values are consistent with those generally produced in polythiophene:fullerene OSCs employing MoO_3 interlayers [30,31]. However, the V_{oc} of OSC-Ref and OSC-MoO_3 are much larger than those obtained for the well-known poly(3-hexylthiophene) (P3HT):PCBM active layers, a reference in the OSC field [22]. This is in accordance with findings from Yao et al., which suggest that P3HTN has a much deeper highest occupied molecular orbital (HOMO) compared to P3HT [25]. Surprisingly, the first and the second voltage scans of OSC-PEDOT:PSS yield very different photo-responsive electrical behaviors. A clear increase in J_{sc} and V_{oc} with respect to OSC-ITO and OSC-MoO_3 can already be observed after the first scan but these photovoltaic parameters are considerably enhanced in the second scan. In particular, an increase in the photocurrent can be observed in the first scan between 0 and 0.3 V. This peculiar behavior is only seen in the devices employing PEDOT:PSS. After the second scan, the *J-V* curves maintain their shapes with some minor changes related to degradation, thus indicating that the observed phenomenon is not easily reversed. Results from the second scan indicate that enhanced J_{sc} and V_{oc} values of 0.546 mA·cm^{-2} and 1.31 V, respectively, can be achieved in OSC-PEDOT:PSS but these devices also exhibit a relatively low *FF* to 33.4%. The differences between the various OSCs and the peculiar shape of the first *J-V* scan of OSC-PEDOT:PSS suggest that some interactions occur at the interface between PEDOT:PSS and the active layer. In particular, as both P3HTN and PEDOT:PSS are polyelectrolytes, our hypothesis is that ion exchanges occur at the interface between the hole collection layer and the active layer, which will considerably influence the optoelectronic properties of these conjugated materials, especially at the bilayer interface.

Table 1. Photovoltaic performances of OSCs employing water-processed P3HTN:PEG-C_{60} thin films.

OSCs	J_{sc} (mA·cm^{-2})	V_{oc} (V)	FF (%)	PCE (%)
OSC-Ref	0.041	0.80	45.4	0.015 ± 0.004
OSC-MoO_3	0.093	0.71	60.1	0.040 ± 0.007
OSC-PEDOT:PSS (2nd)	0.546	1.31	33.4	0.238 ± 0.012

We first verified the impact of such ion exchange on the optical properties of P3HTN by comparing the absorption spectra of P3HTN thin films with those of PEDOT:PSS/P3HTN blends and bilayers (Figure 2). Upon mixing with PEDOT:PSS, we observe a bathochromic shift of the P3HTN absorption maximum from circa 440 nm for P3HTN films to circa 500 nm for the blends. In the bilayers, the P3HTN absorption maximum is only shifted by circa 40 nm. The observed bathochromic shifts can be ascribed to doping of P3HTN by PSS after the counterion exchange occurs. Doping of PEDOT by PSS is a well-documented phenomenon and thus, a similar doping effect can be expected after formation of the ionic complex between P3HTN and PSS [32]. When doped, the absorption of P3HT undergoes a bathochromic shift, which is also associated with the appearance of a new absorption shoulder between 700 and 1000 nm [33,34]. We observe a similar appearance of a new shoulder between 700 and 1000 nm in addition to the bathchromic shift in the P3HTN absorption. These changes clearly support our hypotheses that counterion exchange occurs between PEDOT and P3HTN, and that the changes in P3HTN absorption can be associated with doping effects. As a result, the PEDOT:PSS/P3HTN films can harvest more sunlight due to a better overlap with the maximum of the terrestrial solar spectral irradiance (AM1.5G). These observations are thus consistent with the enhanced J_{sc} produced in these eco-friendly OSCs upon insertion of the PEDOT:PSS layer. The large increase in J_{sc} between the first and the second scans (Figure 1) also suggest that applying an electric field to the device causes the ion exchange to extend to areas further away from the interface.

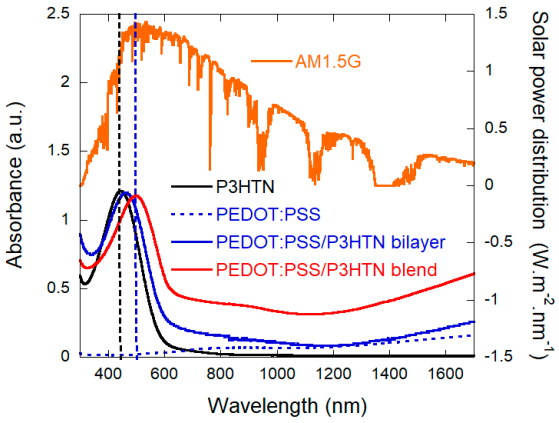

Figure 2. Absorption spectra of P3HTN films, PEDOT:PSS films, PEDOT:PSS/P3HTN bilayers, and PEDOT:PSS/P3HTN blends along with the AM1.5G terrestrial solar irradiance spectrum.

Exchanging the counterion in conjugated polyelectrolytes could also considerably affect the frontier orbitals and hole mobility of the conjugated material. We compared the UPS spectra of P3HTN and PEDOT:PSS/P3HTN bilayers deposited on ITO substrates (Figure 3). In both cases, the work function was found to be 3.76 eV but a clear shift of the ionization potential can be observed with values of 5.30 and 5.88 eV for P3HTN films and PEDOT:PSS/P3HTN bilayers, respectively. The HOMO value for P3HTN films calculated here is consistent with the one measured by Yao et al. using cyclic voltammetry (5.38 eV) [25]. The deeper HOMO of PEDOT:PSS/P3HTN bilayers also correlates well with the larger V_{oc} values produced in OSC-PEDOT:PSS with respect to OSC-Ref. However, such deep HOMO levels can become problematic when it comes to hole collection at the anode and can cause large reductions in *FF*. In fact, a large drop in *FF* can be observed in OSCs employing PEDOT:PSS compared to OSC-MoO_3. The *J-V* curves collected from the hole only devices clearly indicate that there is a mismatch between the work function of the electrodes employing PEDOT:PSS and the HOMO of P3HTN after the ion exchange occurs (Figure 4).

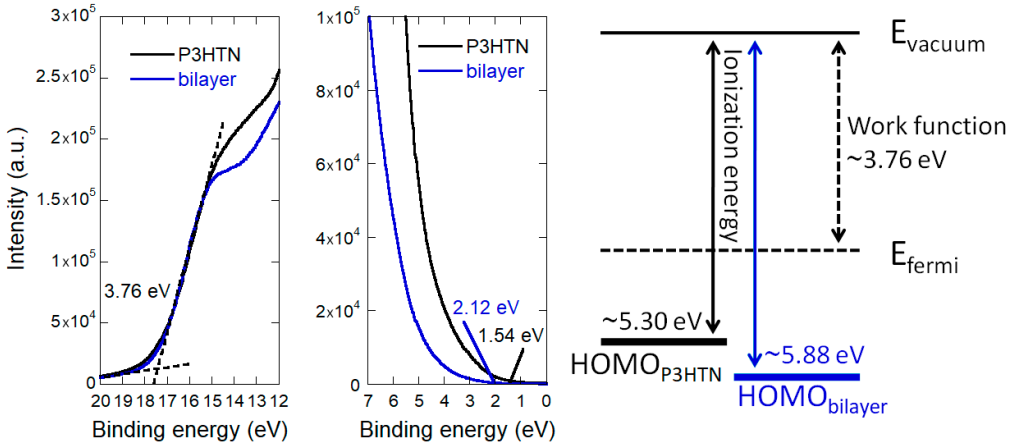

Figure 3. UV photoelectron spectroscopy (UPS) measurements of P3HTN and PEDOT:PSS/P3HTN bilayers deposited on indium tin oxide (ITO) substrates and schematic representation of the deepening of P3HTN highest occupied molecular orbital (HOMO) upon ion exchange with PEDOT:PSS.

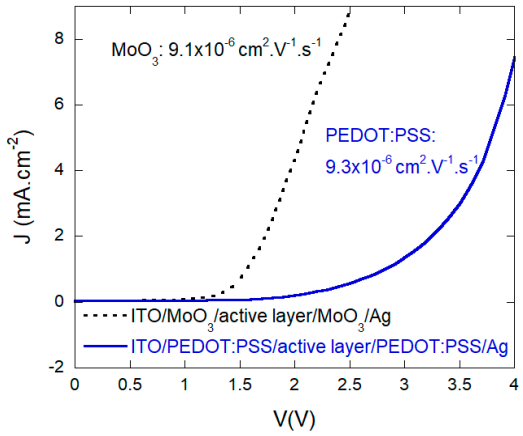

Figure 4. Dark *J-V* characteristics of P3HTN:PEG-C_{60} hole only devices prepared using either MoO_3 or PEDOT:PSS as the hole transporting layer.

The larger hole injection barrier or inefficient hole collection in devices using PEDOT:PSS is reflected by a large increase in the threshold voltage of these hole only devices with respect to those fabricated with MoO_3. On the other hand, the ion exchange only seems to mildly affect the hole mobility in the active layer as devices prepared with PEDOT:PSS and with MoO_3 both yield values around 0.9×10^{-6} $cm^2 \cdot V^{-1} \cdot s^{-1}$ obtained for both devices employing MoO_3 or PEDOT:PSS hole transporting layers. Similar hole mobilities around 1×10^{-6} $cm^2 \cdot V^{-1} \cdot s^{-1}$ can also be measured in devices fabricated without PEG-C_{60}. These relatively low mobility values suggest that increasing the active layer thickness would cause a fast drop in *FF* but also indicate that the ion exchange does not considerably affect the molecular packing of the conjugated polymer.

4. Conclusions

Through this study, we demonstrated that conjugated polyelectrolytes have a great potential for the production of environment-friendly OSCs with V_{oc} largely exceeding 1 V. These high V_{oc} can only be obtained when ion exchanges occur between the polyelectrolyte electron donor (P3HTN) and PEDOT:PSS leading to a stabilization of the P3HTN HOMO level around 5.9 eV. Despite the additional enhancement in light absorption upon ion exchanges at the PEDOT:PSS/active layer interface, the limited active layer thickness obtained in our OSCs is insufficient to harvest a large amount of sunlight. The limited J_{sc} combined with a reduced *FF* resulting from a large hole collection barrier thus leads to low *PCE*s around 0.24%. Nevertheless, our results clearly indicate that conjugated polyelectrolytes have a great potential as electron donors for water-processed high V_{oc} OSCs manufacturing. Future studies to enhance water solubility and hole mobility of conjugated polyelectrolytes, as well as the development of electrodes with adequate work functions should considerably improve the *PCE* of these environment-friendly OSCs. Similar to other OSCs based on polythiophenes and C_{60} derivatives, the eco-friendly devices presented here quickly photo-degrade when operated in air. Replacing the easily photo-oxidized fullerene C_{60} derivatives with the more stable fullerene C_{70} derivatives or with novel water-processable non-fullerene derivatives could be the adequate strategy to increase both the efficiency and stability of water-processed OSC active layers [35,36]. However, unlike water-soluble fullerene C_{60} derivatives, there has not been much research on water-soluble C_{70} derivatives or water-soluble non-fullerene acceptors up to now. Therefore, we should look forward to the development and commercialization of such materials, which could unleash the true potential of water-soluble OSCs based on polyelectrolyte donors.

Author Contributions: Conceptualization, V.V. and Y.T.; methodology, V.V. and Y.T.; formal analysis, V.V. and Y.T.; investigation, V.V. and S.S.; data curation, V.V. and S.S.; writing—original draft preparation, V.V.; writing—review and editing, V.V. and Y.T.; supervision, V.V. and Y.T.; project administration, V.V.; funding acquisition, V.V. and Y.T. All authors have read and agreed to the published version of the manuscript.

Funding: This research was funded by the NF Foundation through the R&D Encouragement Award.

Acknowledgments: The authors would like to acknowledge Takayuki Uchiyama for guiding us through the UPS measurements.

Conflicts of Interest: The authors declare no conflict of interest.

References

1. Lu, L.; Zheng, T.; Wu, Q.; Schneider, A.M.; Zhao, D.; Yu, L. Recent Advances in Bulk Heterojunction Polymer Solar Cells. *Chem. Rev.* **2015**, *115*, 12666–12731. [CrossRef] [PubMed]
2. Yan, J.; Saunders, B.R. Third-generation solar cells: A review and comparison of polymer: Fullerene, hybrid polymer and perovskite solar cells. *RSC Adv.* **2014**, *4*, 43286–43314. [CrossRef]
3. Sharma, K.; Sharma, V.; Sharma, S.S. Dye-Sensitized Solar Cells: Fundamentals and Current Status. *Nanoscale Res. Lett.* **2018**, *13*, 381. [CrossRef]
4. Yuan, M.; Liu, M.; Sargent, E.H. Colloidal quantum dot solids for solution-processed solar cells. *Nat. Energy* **2016**, *1*, 16016. [CrossRef]
5. Vohra, V. Can polymer solar cells open the path to sustainable and efficient photovoltaic windows fabrication? *Chem. Rec.* **2019**, *19*, 1166–1178. [CrossRef] [PubMed]
6. Krebs, F.C. Fabrication and processing of polymer solar cells: A review of printing and coating techniques. *Sol. Energy Mater. Sol. Cells* **2009**, *93*, 394–412. [CrossRef]
7. Li, Y.W.; Xu, G.Y.; Cui, C.H.; Li, Y.F. Flexible and Semitransparent Organic Solar Cells. *Adv. Energy Mater.* **2018**, *8*, 1701791. [CrossRef]
8. Sano, T.; Inaba, S.; Vohra, V. Ternary Active Layers for Neutral Color Semitransparent Organic Solar Cells with PCEs over 4%. *ACS Appl. Energy Mater.* **2019**, *2*, 2534–2540. [CrossRef]
9. Andersen, T.R.; Larsen-Olsen, T.T.; Andreasen, B.; Böttiger, A.P.L.; Carlé, J.E.; Helgesen, M.; Bundgaard, E.; Norrman, K.; Andreasen, J.W.; Jørgensen, M.; et al. Aqueous Processing of Low-Band-Gap Polymer Solar Cells Using Roll-to-Roll Methods. *ACS Nano* **2011**, *5*, 4188–4196. [CrossRef] [PubMed]
10. Ye, L.; Xiong, Y.; Chen, Z.; Zhang, Q.; Fei, Z.; Henry, R.; Heeney, M.; O'Connor, B.T.; You, W.; Ade, H. Sequential Deposition of Organic Films with Eco-Compatible Solvents Improves Performance and Enables Over 12%-Efficiency Nonfullerene Solar Cells. *Adv. Mater.* **2019**, *31*, 1808153. [CrossRef]
11. Fan, Q.; Zhu, Q.; Xu, Z.; Su, W.; Chen, J.; Wu, J.; Guo, X.; Ma, W.; Zhang, M.; Li, Y. Chlorine substituted 2D-conjugated polymer for high-performance polymer solar cells with 13.1% efficiency via toluene processing. *Nano Energy* **2018**, *48*, 413–420. [CrossRef]
12. Lee, J.; Lee, T.H.; Byranvand, M.M.; Choi, K.; Kim, H.I.; Park, S.A.; Kim, J.Y.; Park, T. Green-solvent processable semiconducting polymers applicable in additive-free perovskite and polymer solar cells: Molecular weights, photovoltaic performance, and thermal stability. *J. Mater. Chem. A* **2018**, *6*, 5538–5543. [CrossRef]
13. Tsai, P.-T.; Tsai, C.-Y.; Wang, C.-M.; Chang, Y.-F.; Meng, H.-F.; Chen, Z.-K.; Lin, H.-W.; Zan, H.-W.; Horng, S.-F.; Lai, Y.-C.; et al. High-efficiency polymer solar cells by blade coating in chlorine-free solvents. *Org. Electron.* **2014**, *15*, 893–903. [CrossRef]
14. Meng, B.; Liu, J.; Wang, L. Oligo(ethylene glycol) as side chains of conjugated polymers for optoelectronic applications. *Polym. Chem.* **2020**, *11*, 1261–1270. [CrossRef]
15. Zappia, S.; Scavia, G.; Ferretti, A.M.; Giovanella, U.; Vohra, V.; Destri, S. Water-Processable Amphiphilic Low Band Gap Block Copolymer: Fullerene Blend Nanoparticles as Alternative Sustainable Approach for Organic Solar Cells. *Adv. Sustain. Syst.* **2018**, *2*, 1700155. [CrossRef]
16. Vaughan, B.; Williams, E.L.; Holmes, N.P.; Sonar, P.; Dodabalapur, A.; Dastoor, P.C.; Belcher, W.J. Water-based nanoparticulate solar cells using a diketopyrrolopyrrole donor polymer. *Phys. Chem. Chem. Phys.* **2014**, *16*, 2647–2653. [CrossRef]
17. Prunet, G.; Parrenin, L.; Pavlopoulou, E.; Pecastaings, G.; Brochon, C.; Hadziioannou, G.; Cloutet, E. Aqueous PCDTBT:$PC_{71}BM$ Photovoltaic Inks Made by Nanoprecipitation. *Macromol. RapidCommun.* **2018**, *39*, 1700504. [CrossRef] [PubMed]
18. Vohra, V.; Mróz, W.; Inaba, S.; Porzio, W.; Giovanella, U.; Galeotti, F. Low-Cost and Green Fabrication of Polymer Electronic Devices by Push-Coating of the Polymer Active Layers. *ACS Appl. Mater. Interfaces* **2017**, *9*, 25434–25444. [CrossRef]

19. Inaba, S.; Arai, R.; Mihai, G.; Lazar, O.; Moise, C.; Enachescu, M.; Takeoka, Y.; Vohra, V. Eco-Friendly Push-Coated Polymer Solar Cells with No Active Material Wastes Yield Power Conversion Efficiencies over 5.5%. *ACS Appl. Mater. Interfaces* **2019**, *11*, 10785–10793. [CrossRef]
20. Lee, W.; Seo, J.H.; Woo, H.Y. Conjugated polyelectrolytes: A new class of semiconducting material for organic electronic devices. *Polymer* **2013**, *54*, 5104–5121. [CrossRef]
21. Schmatz, B.; Yuan, Z.; Lang, A.W.; Hernandez, J.L.; Reichmanis, E.; Reynolds, J.R. Aqueous Processing for Printed Organic Electronics: Conjugated Polymers with Multistage Cleavable Side Chains. *ACS Cent. Sci.* **2017**, *3*, 961–967. [CrossRef] [PubMed]
22. Dang, M.T.; Hirsch, L.; Wantz, G. P3HT:PCBM, Best Seller in Polymer Photovoltaic Research. *Adv. Mater.* **2011**, *23*, 3597–3602. [CrossRef] [PubMed]
23. Takeoka, Y.; Saito, F.; Rikukawa, M. Synthesis of optically active regioregularpolythiophenes and their self-organization at the air-water interface. *Langmuir* **2013**, *29*, 8718–8727. [CrossRef] [PubMed]
24. Seo, J.H.; Gutacker, A.; Sun, Y.; Wu, H.; Huang, F.; Cao, Y.; Scherf, U.; Heeger, A.J.; Bazan, G.C. Improved High-Efficiency Organic Solar Cells via Incorporation of a Conjugated Polyelectrolyte Interlayer. *J. Am. Chem. Soc.* **2011**, *133*, 8416–8419. [CrossRef]
25. Yao, K.; Chen, L.; Chen, Y.; Li, F.; Wang, P. Influence of water-soluble polythiophene as an interfacial layer on theP3HT/PCBM bulk heterojunction organic photovoltaics. *J. Mater. Chem.* **2011**, *21*, 13780–13784. [CrossRef]
26. Lanzi, M.; Salatelli, E.; Giorgini, L.; Mucci, A.; Pierini, F.; Di-Nicola, F.P. Water-soluble polythiophenes as efficient charge-transport layers for the improvement of photovoltaic performance in bulk heterojunction polymeric solar cells. *Eur. Polym. J.* **2017**, *97*, 378–388. [CrossRef]
27. Takeoka, Y.; Umezawa, K.; Oshima, T.; Yoshida, M.; Yoshizawa-Fujita, M.; Rikukawa, M. Synthesis and properties of hydrophilic-hydrophobic diblock copolymer ionomers based on poly(*p*-phenylene)s. *Polym. Chem.* **2014**, *5*, 4132–4140. [CrossRef]
28. Sato, T.; Yoshizawa-Fujita, M.; Takeoka, Y.; Rikukawa, M. Formation of polyelectrolyte complexes from cationic polyfluorenes and ssDNA. *J. Anal. Bioanal. Tech.* **2017**, *8*, 388. [CrossRef]
29. Kettle, J.; Waters, H.; Horie, M.; Chang, S.-W. Effect of hole transporting layers on the performance of PCPDTBT:PCBM organic solar cells. *J. Phys. D Appl. Phys.* **2012**, *45*, 125102. [CrossRef]
30. Fan, X.; Fang, G.; Qin, P.; Sun, N.; Liu, N.; Zheng, Q.; Cheng, F.; Yuan, L.; Zhao, X. Deposition temperature effect of RF magnetron sputtered molybdenum oxide films on the power conversion efficiency of bulk-heterojunction solar cells. *J. Phys. D Appl. Phys.* **2011**, *44*, 045101. [CrossRef]
31. Raïssi, M.; Vignau, L.; Cloutet, E.; Ratier, B. Soluble carbon nanotubes/phthalocyanines transparent electrode and interconnection layers for flexible inverted polymer tandem solar cells. *Org. Electron.* **2015**, *21*, 86–91. [CrossRef]
32. Sarath Kumar, S.R.; Kurra, N.; Alshareef, H.N. Enhanced high temperature thermoelectric response of sulphuric acid treated conducting polymer thin films. *J. Mater. Chem. C* **2016**, *4*, 215–221. [CrossRef]
33. Meresa, A.A.; Kim, F.S. Selective Ammonia-Sensing Platforms Based on a Solution-Processed Film of Poly(3-Hexylthiophene) and p-Doping Tris(Pentafluorophenyl)Borane. *Polymers* **2020**, *12*, 128. [CrossRef] [PubMed]
34. Jung, I.H.; Hong, C.T.; Lee, U.-H.; Kang, Y.H.; Jang, K.-S.; Cho, S.Y. High Thermoelectric Power Factor of a Diketopyrrolopyrrole-Based Low Bandgap Polymer via Finely Tuned Doping Engineering. *Sci. Rep.* **2017**, *7*, 44704. [CrossRef] [PubMed]
35. Blazinic, V.; Ericsson, L.K.E.; Muntean, S.A.; Moons, E. Photo-degradation in air of spin-coated $PC_{60}BM$ and $PC_{70}BM$ films. *Synth. Met.* **2018**, *241*, 26–30. [CrossRef]
36. Du, X.; Heumueller, T.; Gruber, W.; Classen, A.; Unruh, T.; Li, N.; Brabec, C.J. Efficient Polymer Solar Cells Based on Non-fullerene Acceptors with Potential Device Lifetime Approaching 10 Years. *Joule* **2019**, *3*, 215–226. [CrossRef]